Available online at www.sciencedirect.com

ScienceDirect

Spectrochimica Acta Part A 67 (2007) 188–195

SPECTROCHIMICA
ACTA
PART A

www.elsevier.com/locate/saa

Spectroscopic techniques and cyclic voltammetry with synthesis: Manganese(II) coordination stability and its ligand field parameters effect on macrocyclic ligands

Rajiv Kumar[a,b,*], Sulekh Chandra[b]

[a] *Department of Chemistry, University of Delhi, New Delhi 110007, India*
[b] *Department of Chemistry, Zakir Husain College, University of Delhi, Jawahar Lal Nehru Marg, New Delhi 110002, India*

Received 11 January 2006; accepted 3 July 2006

Abstract

Manganese(II) macrocyclic complexes are prepared with different macrocyclic ligands, containing cyclic skeleton bearing organic components which have different chromospheres like N, O and S donor atoms and stereochemistry. Thus, six macrocyclic ligands, were prepared and their capacity to retain the manganese(II) ion in solid as well as in aqueous solution was determined and characterized by elemental analyses, molar conductance measurements, magnetic susceptibility measurements, mass, ^{1}H NMR, IR, electronic spectral and cyclic voltammetric studies.

The electronic spectrum of this system showed a dependence that may be consistent with the formation of stable complexes and coordination behaviour of the ions. ESR spectra of all the complexes are recorded in solid as well as solution, which show the oxidation state of the manganese(II). Spin Hamiltonian manganese(II), which can be defined as the magnetic field vector ($\mathscr{H}$):

$$\mathscr{H} = g\beta_e HS + D\left[S_z^2 - \frac{35}{12}\right] + E[S_z^2 - S_y^2] + ASI + \frac{1}{6}a$$

$$\left[S_x^4 + S_y^4 + S_z^4 - \frac{707}{16}\right] + \frac{1}{180}F\left[\frac{35S_z^2 - 475}{2S_z^2 + 3255/10}\right]$$

Significant distortion of the manganese(II) ion in observed geometry is evident from the angle subtended by the different membered chelate rings and the angles spanned by trans donor atoms octahedral geometry. Cyclic voltammetric studies indicate that complexes with all ligands undergoes one electron oxidation from manganese(II) to manganese(III) followed by a further oxidation to manganese(IV) at a significantly more positive potential.

Keywords: Macrocyclic ligands; EPR; IR; Cyclic voltammetry; Mn(II)complexes

1. Introduction

Manganese and its compounds find very historical importance in medicine and also have some biological importance. Manganese plays a significant role in enzyme activation. Citrate cyclase catalyzes the cleavage of citrate to oxaloacetate and acetate in the presence of manganese(II) or magnesium(II) [1]. In order to obtain new model of such complexes, here we are able to develop such different chromospheres containing organic cyclic ligands as reported earlier [2–5].

It is well known that manganese plays an important role in many biological redox processes including disproportionation of hydrogen peroxide (catalase activity) in micro-organisms [6], decomposition of O_2^- radicals catalyzed by superoxide dismutases (SODs) [7] and water oxidation by photosynthetic enzymes (photosystem II) [8]. Superoxide dismutase catalyses the dismutation of superoxide radical anions to the non-radical products oxygen and hydrogen peroxide and protects the living cells against the toxicity of hydroxia [9] $O_2^- + H_2O + H^+ \rightarrow O_2 + H_2O_2$.

---

[*] Corresponding author. Tel.: +91 1234276530; fax: +91 1234276530.
E-mail address: chemistry_rajiv@hotmail.com (R. Kumar).

1386-1425/$ – see front matter © 2006 Elsevier B.V. All rights reserved.
doi:10.1016/j.saa.2006.07.001

Also manganese(II) can replace magnesium(II) in a number of biological system [10–13]. A number of reviews are available on the physiology and biochemistry of manganese in mammals [14]. DNA and RNA polymerases [15] catalyze the replication and transcription of DNA, have a specific requirement for manganese(II). The binding of manganese(II) in these systems have been characterized by the using EPR. There are some examples of enzymes, which bind manganese tightly such as pseudocatalase [16], ribonucleotide reducatse [17,18] and oxygen evolving centre in photosystem-II [19]. On the basis of above importance which manganese has in biological systems? The synthesis and characterization studies on macrocyclic complexes of manganese(II) are highly desirable with these six macrocylic ligands: 2,4,10,12-tetraphenyl-1,5,7,9,13,15-hexaazatricyclo[15,3,1]-octadeca-1, 4,7,9,12,14-hexaene[*N*$_6$]ane(L^1); 2,4,10,12-tetraphenyl-1,5,7, 13,-tetraazacyclohexadeca-1,4,9,12-teraene [*N*$_4$]ane (L^2);2,4, 9,11-tetraphenyl-1,5,8,12-tetraazacycloteradeca-1,4,8,11-tetraene[*N*$_4$]ane (L^3); 1,4,7,10,13,16-hexaaza-cyclooctadecane[*N*$_6$] ane (L^4); 1,8-diaza-4,5,11-trithia-2,3:6,7-dibenzo[*b*,*h*]-cyclopentadeca-9,13-dione[*S*$_3$*N*$_2$]ane (L^5); 9,18-dimethyl-1,7,10,16-tetraza-4,13-dithia-cyclooctadecane-2,6,11,16-teraone (L^6).

2. Experimental

All the chemicals used were of AnalaR grade and procured from Fluka. Metal salts were purchased from E. Merck and were used as received. All solvents used were purified before use according to standard procedures.

2.1. Physical measurements

C, H and N were analysed on a Carlo-Erba 1106 elemental analyzer. Molar conductances were measured on an Elico (CM82T) conductivity bridge. Magnetic susceptibilities were measured at room temperature on a Gouy balance using $CuSO_4{\cdot}5H_2O$ as a calibrant. Electron impact mass spectra were recorded on a Jeol, JMS, DX-303 mass spectrometer. ^{1}H NMR spectra were recorded on a model R-600 Hitachi FT-NMR, model R-600 spectrometer using deuterated DMF as solvent, chemical shifts are given in ppm relative to tetramethylsilane. IR spectra (KBr) were recorded on a FTIR Spectrum BX-II spectrophotometer. The electronic spectra were recorded in DMSO on a Shimadzu UV mini-1240 spectrophotometer. EPR spectra of the complexes were recorded as polycrystalline samples and in solution in DMSO at room temperature for maganease(II) complexes on an E_4 EPR spectrometer using DPPH as the g-marker. Cyclic voltammetry of the complexes was recorded in DMF at a scan rate of $100\,mV\,s^{-1}$. The redox potential was recorded with Ag/AgCl as reference electrode and platinum as working electrode, tetrabutylammonium phosphate was the supporting electrolyte.

The $E_{0.5}$ values were also equal to the $E_{0.5}$ values measured under steady-state conditions at a microelectrode as the potential at half the limiting current value ($I_L/2$).

2.2. Isolation and preparation of macrocyclic ligands

Ligand L^2, L^4, L^5 and L^6 are prepared and characterized as reported earlier [2–5]. Ligand L^1 and L^3 were synthesized by refluxing an ethanolic solution of dibenzoylmethane (0.01 mol) with an ethanolic solution of 2,6-diaminopyridine or diaminoethane (0.01 mol) for 5 h in the presence of few drops of conc. HCl. On cooling the contents overnight a dull white crystalline compound separated out. This was filtered, washed with ethanol and dried over P_4O_{10}. Molecular formula (L^1): $C_{40}H_{30}N_6$ (Found: C% = 80.20, H% = 4.92, N% = 30.91, Calcd. C% = 80.81, H% = 5. 05, N% = 14.13). Molecular formula (L^3): $C_{36}H_{36}N_4$ (Found: C% = 81.80, H% = 6.13, N% = 10.91, Calcd. C% = 82.25, H% = 6. 45, N% = 11.28).

2.3. Characterization of macrocyclic ligands

2.3.1. ^{1}H NMR spectra of macrocyclic ligands

These ligands are characterized on the basis of elemental analysis, mass spectra and infrared spectra. The electron impact mass spectra of the ligands confirm the proposed formula by showing different peaks corresponding to the macrocyclic moiety corresponding to various fragments. Their intensity revealed the stability of these fragments. The ^{1}H NMR spectra of the ligand (L^1 and L^3) do not show signal corresponds to primary amine and ethyl protons. Other signals appear in the regions at 1.53 and 7.22 ppm. These signals correspond to methyne (–CH–CH_2–) and benzenoid protons, respectively.

2.3.2. IR spectra of macrocyclic ligands

IR spectral studies of isolated ligands show different characteristic bands according their functional group present. The main characteristic, strong band >C=N lies in the range of 1599–1628 cm^{-1}. This band confirms the reaction between primary amine group –NH_2 of diamine and carbonyl group of diketone or any other carbonyl compounds. So the bands due to –NH_2 group of diamine in 3200–3350 cm^{-1} region and >C=O group of carbonyl compounds above 1700 cm^{-1} are absent. These confirm the elimination of water molecule and also confirm complete condensation. The absorptions in the IR spectrum of L^3 in the range of 720–780 and 1430–1630 cm^{-1} are due to the presence of a phenyl group. IR spectrum shows a new medium to strong band in region 1531–1465 cm^{-1} as expected for the highest energy pyridine ring vibrations. IR spectra of all ligands show a strong band in region 2950–3010 cm^{-1}, which confirms the C–H stretching due to the –CH_2– group. The ligand may be racemic or meso; however, this will not affect the geometry of the complexes. Thin-layer chromatography has been performed which indicates that the ligand is not a mixture (Fig. 1).

2.4. Preparation of manganese(II) complexes (1 + 1) condensation

A hot ethanolic solution (20.0 ml) of $MnCl_2$ or $Mn(SCN)_2$ is added to the ethanolic solution (20.0 ml) of ligand. The mixture was refluxed on water bath at 65 °C for 4–5 h. The color of the solution changed in to pale yellow, off white and brown

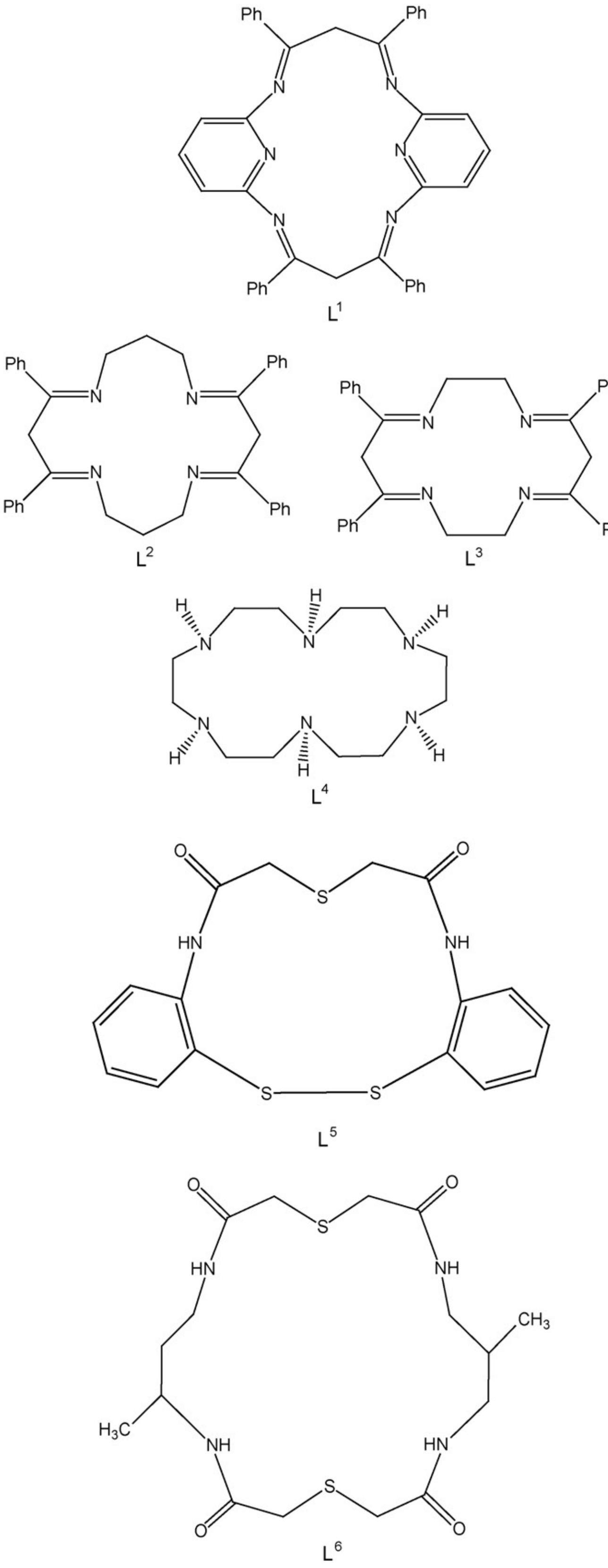

Fig. 1. Structure of the macrocyclic ligands.

according macrocyclic ligands. On cooling, precipitate, so obtained, filtered, washed with ethanol and dried over P_4O_{10} under vacuum.

3. Result discussion

On the basis of elemental analysis, complexes under study were found to have general composition MLX_2 (L = ligand and X = Cl^-, SCN^- and $1/2SO_4{}^{2-}$) and related data are presented in Table 1.

Chloro complexes of L^2, and L^3 are non-electrolytes but the chloro complexes of ligands L^1, L^4, L^6 and L^5 are 1:2 and 1:1 electrolytes, respectively. Thiocyanato complexes of ligands L^2 and L^3 are non-electrolytes but complexes of ligands L^1, L^4, L^6 and L^5 are 1:2 and 1:1 electrolytes, respectively. Thus, the complexes may be formulated as $[MnLX_2]$ $[MnLX]X$, and $[MnL]X_2$.

3.1. *IR spectra*

IR spectra of chloro complexes of all ligands show that the shifting in >C=N band to lower side in most complexes. It confirms, the coordination takes place between the metal ion and donating atoms.

3.1.1. *Confirmation and coordination ability of sulphato anion by IR spectra*

Spectral studies of ligands L^1 and L^6 sulphato complexes show the sharp band in the range 1101–1115 cm^{-1}, which shows ionic behaviour or uncoordinate sulphate of sulphato group. According to Nakamoto [20] ionic sulphato group belongs to high symmetry point groups T_d and shows two bands at 1104 and 613 cm^{-1} denoted as ν_3 and ν_4 do not split and ν_2 do not appear, although if observed, it is very weak. He suggests ν_3 appeared at approximately 1104 cm^{-1} and weak band 613 cm^{-1} for ionic sulphate.

Sulphato complex of L^5 shows that ν_3 band at 1030–1140 cm^{-1}(s) and other in the range 604–645 cm^{-1}(ν_4). This indicates unidentate behaviour of sulphate group [21]. According to Nakamoto [20] monodentate sulphate group belongs to C_{3v} symmetry and shows bands with medium intensity, moreover, ν_3 and ν_4 each splits in to two bands. This result can be explained by assuming a lowering of symmetry from T_d to C_{3v} (unidentate co-ordination).

3.1.2. *Confirmation and coordination ability of pseudohalide anion by IR spectra*

Coordination ability of thiocyanate ion, which is also, called pseudohalide ion. This ion may coordinate to a metal through either one of the end atoms. It may be bonded to metal ion through sulphur atom or nitrogen atom. As a result two linkage isomers are possible, one is M–SCN, which is brown as thiocyanate complexes and second is M–NCS, which is known as isothiocyanato complexes.

In general, first transition form M–N bonded whereas second and third transition series form M–S-bonded [22]. The CN stretching frequencies are observed in L^5 complex near

Table 1
Molar conductance and elemental analyses data of the manganese(II) complexes

Complexes/empirical formula	Yield (%)	Molar conductance (Ω^{-1} cm^2 mol^{-1})	Color	Elemental analysis calculated (found) (%)			
				Mn	C	H	N
$[Mn(L^1)]Cl_2/MnC_{40}H_{30}N_6Cl_2$	70	198.0	Brown	7.64 (7.14)	66.70 (66.12)	4.17 (3.84)	11.67 (11.17)
$[Mn(L^1)]SO_4/MnC_{40}H_{30}N_6SO_4$	40	95.0	White	7.35 (6.85)	64.45 (64.00)	4.04 (3.74)	11.27 (10.83)
$[Mn(L^1)](SCN)_2/MnC_{42}H_{30}N_8S_2$	47	190.0	White	7.18 (6.75)	65.89 (64.19)	3.92 (3.34)	25.61 (24.11)
$[Mn(L^2)Cl_2]/MnC_{36}H_{36}N_4Cl_2$	65	14.0	Brown	8.45 (8.15)	66.49 (61.12)	5.54 (5.16)	8.62 (8.12)
$[Mn(L^3)Cl_2]/MnC_{34}H_{32}N_4Cl_2$	62	17.0	Reddish brown	8.83 (8.49)	65.60 (65.42)	5.18 (5.15)	9.00 (8.55)
$[Mn(L^4)]Cl_2/MnC_{12}H_{30}N_6Cl_2$	66	205.0	Off brown	14.30 (13.8)	37.53 (37.12)	7.82 (7.26)	21.88 (21.34)
$[Mn(L^5)Cl]Cl/MnC_{18}H_{18}N_2S_3O_2Cl_2$	61	105.0	Brown	10.64 (10.51)	41.88 (41.62.)	3.48 (3.18)	5.42 (5.12)
$[Mn(L^5)SO_4]/MnC_{18}H_{18}N_2S_4O_6$	52	15.0	Black brown	10.15 (9.91)	39.94 (39.84)	3.33 (3.21)	5.44 (5.24)
$[Mn(L^5)(SCN)](SCN)/MnC_{22}H_{22}N_4S_5O_3$	47	92.0	White	9.79 (9.65)	42.79 (42.61)	3.21 (2.99)	9.97 (9.88)
$[Mn(L^6)]Cl_2/MnC_{14}H_{24}N_4S_2O_4Cl_2$	35	201.0	White	10.94 (10.75)	33.49 (33.28)	4.78 (4.61)	11.15 (10.82)
$[Mn(L^6)]SO_4/MnC_{14}H_{24}N_4S_2O_8$	71	106.0	Brown	10.42 (10.26)	31.90 (31.71)	4.55 (4.25)	10.62 (10.51)
$[Mn(L^6)](SCN)_2/MnC_{16}H_{24}N_6S_4O_4$	60	195.0	White	10.04 (9.91)	35.11 (34.98)	4.39 (4.21)	15.35 (15.15)

2070 cm^{-1}, which is corresponds to N-bonded behaviour of this group but the thiocyanate complexes of ligands L^1 and L^6 under study show ionic behaviour of thiocyanato group or uncoordinate nature of this group [23].

3.2. *Magnetic moment*

The ground state term of manganese(II) is $^6A_{1g}$. There is no temperature-independent paramagnetic effect and no reduction of the moment below the spin only value by spin–orbit coupling with higher ligand filed terms. Magnetic movement of the complexes recorded at room temperature (298 K). The present complexes show magnetic moment in the range 5.85–6.02 BM, which are corresponding spin-only values, suggesting an octahedral geometry around manganese ion. Magnetic moment calculated from the susceptibility measurements after correcting diamagnetic contribution [24,25]. Magnetic moment values of the complexes under study are given in Table 2.

3.3. *Electronic spectra of manganese(II) complexes*

The electronic spectra of the manganese(II) complexes exhibit four weak-intensity absorption bands in the ranges 17280–18,950; 23,923–28,380; 28,450–28,980; 31,055–31,600 cm^{-1}, which may be assigned to the transitions: $^6A_{1g} \rightarrow {}^4T_{1g}(^4G)$, $^6A_{1g} \rightarrow {}^4E_g$, $^4A_{1g}(^4G)$ (10B + 5C), $^6A_{1g} \rightarrow {}^4E_g(^4D)$ (17B + 5C) and $^6A_{1g} \rightarrow {}^4T_{1g}(^4P)$ (7B + 7C), respectively[2,26].

3.3.1. *Ligands field parameters of manganese(II) complexes*

The parameters *B* and *C* were calculated and reported which have a good agreement with data reported earlier [24]. The calculated values of the ligand field parameters are given in Table 3. These values are calculated from the second and third transitions because these transitions are free from the crystal field splitting and depend on *B* and *C* parameters. Orgen [27] calculate the values of D_q with the help of curve, transition energies versus D_q, as given by the using the energy due to the transition $^6A_{1g} \rightarrow {}^4T_{1g}$ (^{4}G). Parameters *B* and *C* are linear combinations of certain coulombs and exchange integral, which are generally, treated empirical parameters obtained from the spectra of the free ions. Slater Condon-shortly repulsion parameters F_2 and F_4 are related to Racah parameters *B* and *C* as: $B = F_2 - 5F_4$ and $C = 35F_4$, The electron–electron repulsion in the complexes is more than in the free ion, resulting in an increased distance between electrons, and thus, affects the size of the orbital. On

Table 2
Magnetic moment and electronic spectra of the manganese(II) complexes with L^1 and L^2

Complex	μ efficiency (BM)	υ_1 (cm^{-1})	υ_2 (cm^{-1})	υ_3 (cm^{-1})	υ_4 (cm^{-1})
$[Mn(L^1)]Cl_2$	5.89	17,750	24,200	28,600	–
$[Mn(L^1)]SO_4$	5.98	17,300	24,650	28,950	31,600
$[Mn(L^1)](SCN)_2$	5.93	17,950	24,700	28,980	–
$[Mn(L^2)Cl_2]$	5.89	18,950	24,300	28,740	–
$[Mn(L^3)Cl_2]$	5.89	17,950	23,923	27,840	–
$[Mn(L^4)]Cl_2$	6.02	18,867	24,449	28,901	31,055
$[Mn(L^5)Cl]Cl$	6.01	17,600	24,850	28,900	32,000
$[Mn(L^5)SO_4]$	6.00	17,900	24,810	28,200	31,800
$[Mn(L^5)(SCN)](SCN)$	5.99	17,660	24,800	28,980	–
$[Mn(L^6)]Cl_2$	5.95	17,280	24,100	28,650	31,400
$[Mn(L^6)]SO_4$	5.8	18,540	28,380	28,750	–
$[Mn(L^6)](SCN)_2$	5.8	17,600	24,950	28,450	–

Table 3
Ligand field parameters of the manganese(II) complex

Complex	D_q (cm^{-1})	B (cm^{-1})	C (cm^{-1})	β	F_4	F_2	hx
$[Mn(L^1)]Cl_2$	1775	628	3584	0.79	102	1138	3.00
$[Mn(L^1)]SO_4$	1780	614	3702	0.78	105	1139	4.00
$[Mn(L^1)](SCN)_2$	1730	611	3694	0.77	105	1136	3.28
$[Mn(L^2)Cl_2]$	1795	634	3592	0.80	102	1144	3.86
$[Mn(L^3)Cl_2]$	1795	560	3664	0.69	104	1080	4.40
$[Mn(L^4)]Cl_2$	1886	636	3617	0.80	103	1151	2.80
$[Mn(L^5)Cl]Cl$	1830	617	3682	0.78	105	1142	3.14
$[Mn(L^5)SO_4]$	1760	484	3994	0.61	114	1054	5.57
$[Mn(L^5)(SCN)](SCN)$	1790	597	3766	0.75	107	1132	3.57
$[Mn(L^6)]Cl_2$	1766	650	3520	0.82	100	1150	2.57
$[Mn(L^6)]SO_4$	1828	624	3628	0.79	103	1139	3.00
$[Mn(L^6)](SCN)_2$	1854	500	3990	0.63	114	1074	5.29

increasing delocalization, the value of β decreases up to less than one in the complexes.

The value of β can be calculated from the Nephelauxetic parameter for the ligand (hx) and the Nephelauxetic parameter for the metal ion (km) as $(1-\beta) = \text{hx} \times \text{km}$. The value of the parameter hx for manganese(II) complexes have been calculated by using the co-valency contribution of manganese(II), while for the calculation of β, we used the numerical value of B for manganese(II) free ion which is 786 cm^{-1}. The observed values for parameter β and hx suggest that the complexes, reported here, have appreciable ionic character [28].

3.4. EPR spectra of manganese(II) complexes

EPR spectra were recorded at room temperature for a polycrystalline sample as well as DMSO and calculated data are reported in Table 4. Ground term of manganese(II) high spin is $^6S_{5/2}$. However, the combined action of the electric field gradient and the spin–spin interaction produces splitting of the energy levels due to second order spin–orbital coupling between the ^6A_1g ground state and the lowest level of the ^4A_2g state [29]. For a weak crystal field (t_{2g} Eg^2, $S = 5/2$) the EPR results on d^5 ions have fitted to the spin Hamiltonian manganese(II) which can be defined as

$$\mathcal{H} = g\beta_e HS + D\left[S_z^2 - \frac{35}{12}\right] + E\,[S_z^2 - S_y^2] + ASI + \frac{1}{6}a$$

$$\left[S_x^4 + S_y^4 + S_z^4 - \frac{707}{16}\right] + \frac{1}{180}F\left[\frac{35S_z^2 - 475}{2S_z^2 + 3255/10}\right]$$

where $\mathcal{H}$ is the magnetic field vector, g the spectroscopic splitting factor, β the Bohr magnetron, A the manganese hyperfine splitting constant, S the electron spin vector, I the nuclear spin vector, $S = 5/2$ and S_z is the diagonal spin operator.

Further, a resonance is readily detected even for large zero-field splitting, because d^5 is an odd-electron system whose ground state is a Kramer's doublet and whose degeneracy is only completely removed by a magnetic field. In polycrystalline samples, manganese(II) complexes usually gives broad signals attributed to forbidden transitions where $\Delta m = \pm M$ (M = electron spin quantum number) and $\Delta m \neq 0$ (m = nuclear spin quantum number).

The broadening of the spectrum in powder sample is analogous to that observed in the case of immobilized free-radicals, e.g. manganese(II) complexes of Concanavalin broadening due to immobilization of $M = \pm M$ ion in the ligand results because the rotational motion of manganese(II) is highly restricted.

In DMSO solution, the manganese(II) complexes give EPR spectra containing the six lines arising due to the hyperfine interaction between the unpaired electron with the ^{55}Mn nucleus ($1 = 5/2$). The nuclear magnetic quantum number M_1, corresponding to these lines, are −5/2, −3/2, −1/2, +1/2, +3/2 and +5/2 from low to high field [2,30] (Figs. 2–4).

Table 4
EPR parameters of the manganese(II) complex

Complex	$g_\parallel$	$g_\perp$	A_0	g_{iso}
$[Mn(L^1)]Cl_2$	3.95	1.89	111	2.58
$[Mn(L^1)]SO_4$	3.64	1.87	110	2.46
$[Mn(L^1)](SCN)_2$	3.94	1.99	105	2.64
$[Mn(L^2)Cl_2]$	3.77	1.91	103	2.69
$[Mn(L^3)Cl_2]$	3.99	1.93	108	2.66
$[Mn(L^4)]Cl_2$	3.95	1.89	109	2.58
$[Mn(L^5)Cl]Cl$	3.65	1.87	110	2.46
$[Mn(L^5)SO_4]$	3.94	1.99	121	2.64
$[Mn(L^5)(SCN)](SCN)$	3.99	1.99	118	2.66
$[Mn(L^6)]Cl_2$	3.93	1.95	117	2.65
$[Mn(L^6)]SO_4$	3.91	1.96	113	2.63
$[Mn(L^6)](SCN)_2$	3.98	1.98	114	2.64

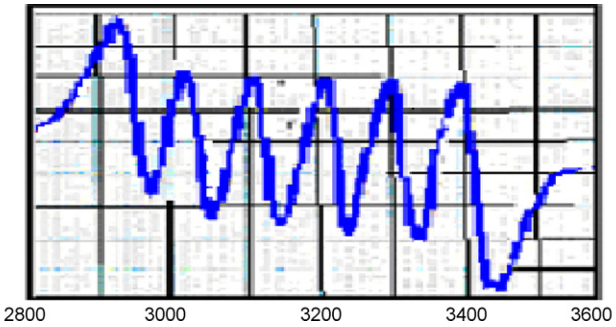

Fig. 2. EPR spectrum of $Mn(L^1)Cl_2$.

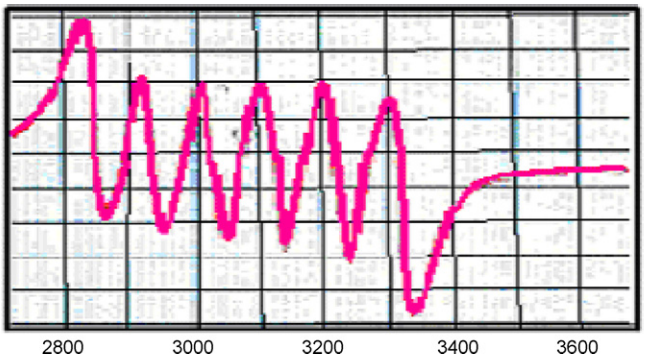

Fig. 3. EPR spectrum of Mn(L^4)Cl_2.

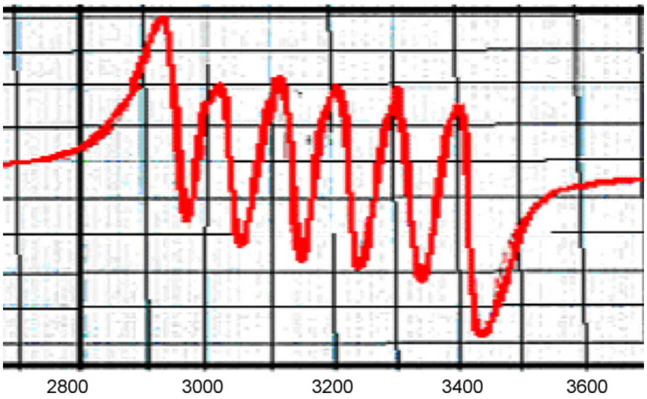

Fig. 4. EPR spectrum of Mn(L^5)Cl_2.

4. FAB mass spectrum

The FAB mass spectrum gives additional structural information about the stereochemistry of the studies complexes. The FAB mass spectrum of $MnC_{34}H_{32}N_4Cl_2$ shows a molecular ion (M^+) peak at $m/z = 384.25$ a.m.u., which suggests the monomeric nature of the complex and confirm the proposed formula. The spectrum of complex also shows a series of peaks corresponding to various fragments. Their intensity gives an idea of the stability of the fragments and also about the geometrical configuration.

5. Redox behaviour by cyclic voltammetry measurements

The redox behaviour of all the complexes displays a chemically reversible wave at a scan rate of 100 mV s^{-1}. This $E_{0.5}$ value is assumed to be the reversible potential because it is in agreement with the E_p. In the cyclic voltammetry measurements, the oxidation of manganese(II)/manganese(III) state in two unresolved one electron processes [Mn(II) → Mn(II)Mn(III) → Mn(III)] and then to the manganese(IV) state [Mn(III) → Mn(III)Mn(IV) → Mn(IV)].

CV signals are relatively sharp compared to those for these complexes, as evidenced by the smaller ΔE_p values of 72 and 78 mV, respectively. However, these ΔE_p values are still larger than expected for a simultaneous two electron process (i.e., $\Delta E_p = 57$ mV/n), indicating that oxidation of the two manganese(II) centers to manganese(III) occurs via two closely spaced one electron processes, but with a separation of 25 ± 10 mV.

The average $E_{0.5}$ values for the first unresolved two electrons oxidation responses of L^1, L^4, L^5 and specially L^6 decrease with increasing $E_{1/2} = +0.55$ to $+0.48$ V according to chain length as do those for the second oxidation +1.33 to +1.23 V. The investigated data explain the probability that, as the alkyl chain has a slight effect on cyclic potentials of metal centre [4]. These complexes show ($E_{0.5}$ values of +0.41 and +1.03 V), which reflects the absence of electrostatic effects that would be caused by a second metal center in large ring containing macrocyclic ligands systems. The aromatic part of such ligands systems may be reducing the binding ability of the bridgehead nitrogen and hence the overall field strength of the ligand, and this could be creating problems in oxidation process in the complexes of L^1, L^2, L^3, L^5, L^6 comparatively L^4.

Acknowledgements

One of the authors (Rajiv Kumar) gratefully acknowledges his younger brother Bitto for motivation. Specially, thanks to Mohit Krishan, Computer Programmer, CSL Delhi University Delhi for providing computer facilities. Thanks to the University Grants Commission, New Delhi for financial assistance. Thanks

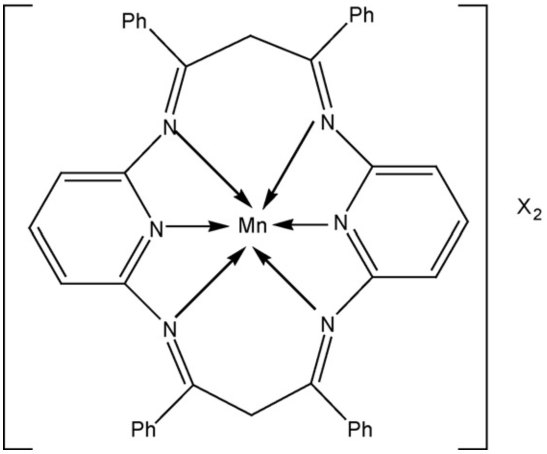

Fig. 5. Structure of [MnL^1]Cl_2 complex where (X = Cl).

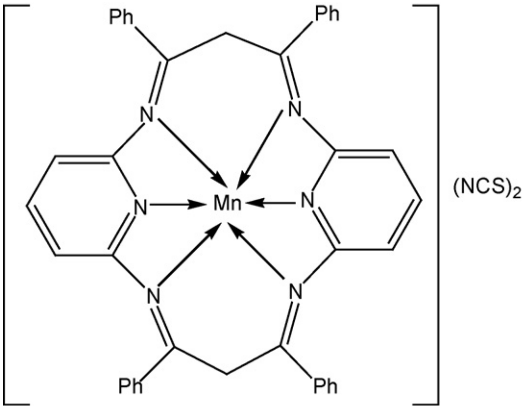

Fig. 6. Structure of [MnL^1]$(NCS)_2$ complex.

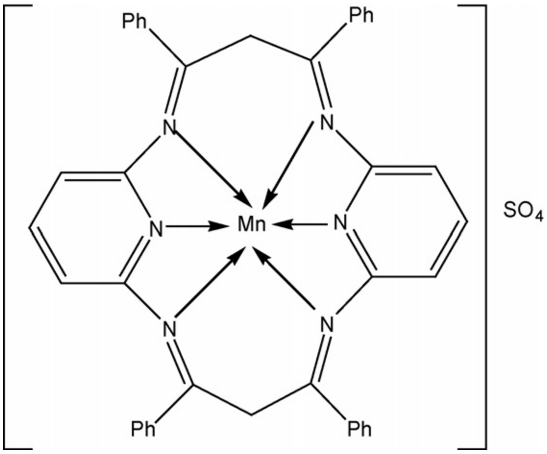

Fig. 7. Structure of [MnL^1]SO$_4$ complex.

to IIT Bombay for recording EPR spectra. Thanks are also due to the Solid State Physics Laboratory, India for recording magnetic moments.

Thus, on the basis of above discussion which is based upon elemental analysis, molar conductance, magnetic susceptibility, IR, electronic, EPR spectral studies, the following structures are investigated for the complexes (Figs. 5–15).

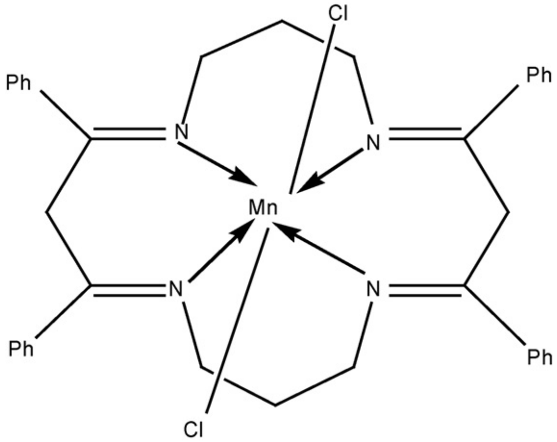

Fig. 8. Structure of [MnL^{2}Cl$_2$] complex.

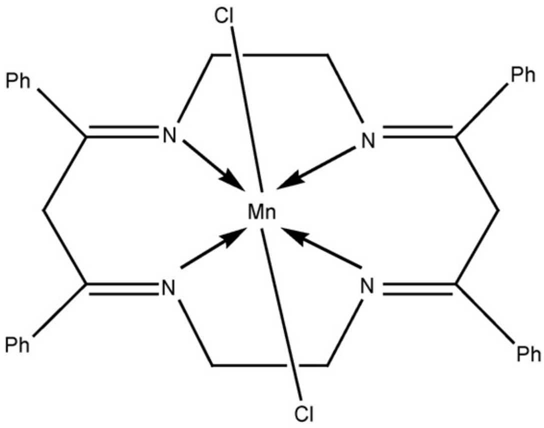

Fig. 9. Structure of [MnL^{3}Cl$_2$] complex.

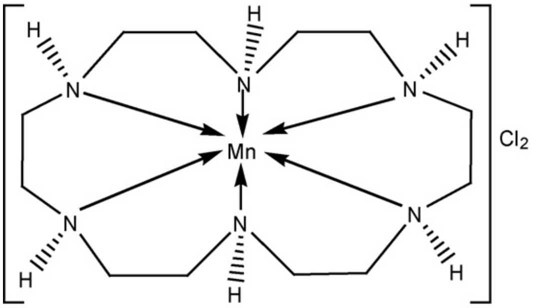

Fig. 10. Structure of [MnL^{4}Cl$_2$] complex.

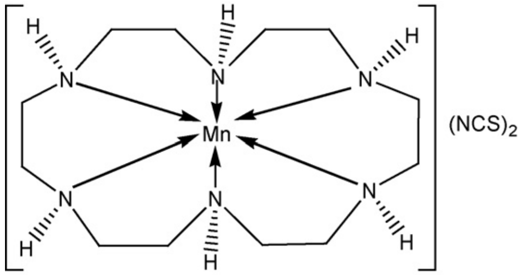

Fig. 11. Structure of [MnL^4(NCS)$_2$] complex.

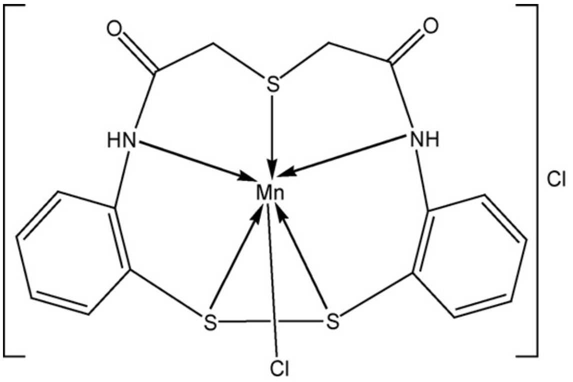

Fig. 12. Structure of [MnL^{5}Cl]Cl complex with L^5.

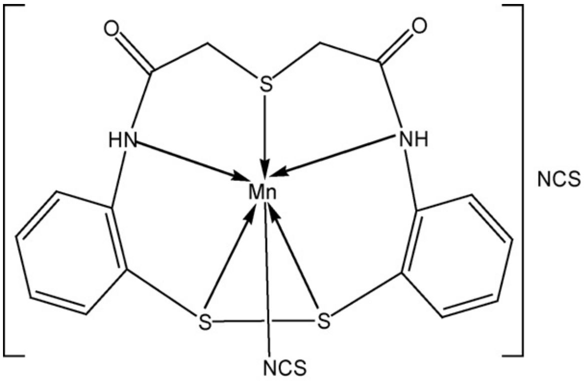

Fig. 13. Structure of [MnL^5(NCS)]NCS complex.

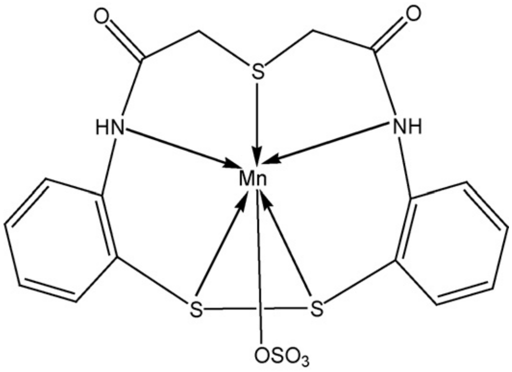

Fig. 14. Structure of $[MnL^5SO_4]$ complex.

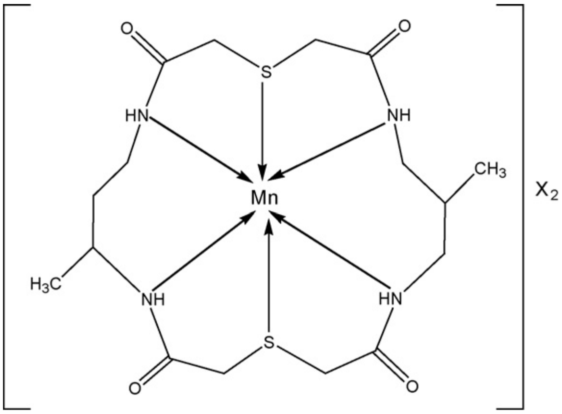

Fig. 15. Structure of $[MnL^6]X_2$ complex, where X = NCS, CI and NO_3.

References

[1] H. Sigel (Ed.), Metal Ions in Biological Systems, vol.13, Marcel Dekker, New York, 2002, p. p981.
[2] S. Chandra, R. Kumar, Trans. Met. Chem. 29 (2004) 269.
[3] S. Chandra, R. Kumar, Synth. React. Inorg. Met. Org. Nano-Met. Chem. 35 (2005) 103.
[4] S. Chandra, R. Kumar, Synth. React. Inorg. Met. Org. Nano-Met. Chem. 35 (2005) 161.
[5] S. Chandra, R. Kumar, Spectrochim. Acta Part A 61 (2005) 437.
[6] S. Chandra, R. Kumar, Spectrochim. Acta Part A 62 (2005) 518.
[7] M.L. Ludwig, K.A. Pettridge, W.C. Stallings, Manganese in Metabolism and Enzyme Function, Academic Press, New York, 1986 (p. 405, Chapter 21).
[8] G.C. Dismukes, Photochem. Photobiol. 43 (1986) 99.
[9] I. Fridovich, Acc. Chem. Res. 15 (1982) 200.
[10] R.C. Valeutine, B.M. Shapire, E.R. Stadtman, Biochemistry 7 (1968) 2143.
[11] M.B. Druton, A.J. Gimberg, Vired. 1 (1967) 97.
[12] E.M. Martin, J.A. Sonuabend, J. Vired. 1 (1967) 97.
[13] U. Maitra, J. Nakatay, J. Hurwitez, J. Biol. Chem. 242 (1967) 4098.
[14] R.M. Leach, M.S. Lilburn, World Rev. Nutr. Diet 32 (1978) 123.
[15] V.L. Pecoraro, Photochem. Photobiol. 48 (1988) 249.
[16] Y. Kono, I. Fridovrich, J. Biol. Chem. 250 (1983) 6015.
[17] G. Schimpff-Weiland, H. Fallmann, G. Auling, Biochem. Biophys. Res. Commun. 102 (1981) 1276.
[18] M. Lammens, H.H. Follman, Struct. Bond. (Berlin) 84 (1983) 27.
[19] J. Livorness, T.D. Smith, Struct. Bond. (Berlin) 48 (1982) 1.
[20] K. Nakamoto, Infrared and Raman Spectra of Inorganic and Coordination Compounds, A Wiley–Interscience Publications, New York, 1977, p. 239.
[21] F.N. Tebbe, G.W. Parshall, J. Am. Chem. Soc. 93 (1971) 3793.
[22] K. Nakamoto, Infrared and Raman spectra of Inorganic and coordination compounds, A Wiley–Interscience Publications, New York, 1977, p. 270.
[23] N.B. Colthup, L.H. Dally, S.E. Wiberley, Introduction to Infrared and Raman Spectroscopy, Academic Press, New York, 1963.
[24] B.N. Figgis, Introduction to Ligand Field Theory, Wiley–Interscience, New York, 1978.
[25] R.L. Carlin, Magnetochemistry, vol. 41A, Springer-Verleg, New York, 2002, p. 1821.
[26] A.B.P. Lever, Inorganic Electronic Spectroscopy, Elsevier, Amsterdam, 1968.
[27] I.F. Orgen, J. Chem. Phys. 23 (1955) 1004.
[28] J.E. Hyheey, Principles of Structure and Reactivity, vol. 363, Harper and Row, New York, 1972.
[29] C.K. Jorgenson, Oxidation Number and Oxidation State, Springer, New York, 1969, p. 106.
[30] A.S. Chakravorty, J. Chem. Phys. 39 (1963) 10004.